Decay schemes for high-spin states in ^{42}K and ^{42}Ca†

E. K. Warburton, J. J. Kolata, and J. W. Olness
Brookhaven National Laboratory, Upton, New York 11973
(Received 5 November 1974)

Fusion-evaporation reactions induced by ^{18}O and ^{19}F bombardment of ^{26}Mg, ^{27}Al, and ^{28}Si targets with projectile energies of 20–60 MeV were used to populate high-spin states in ^{42}K and ^{42}Ca. Ge(Li) measurements of γ-γ coincidences, together with γ-ray angular distribution and linear polarization measurements, were used to establish decay schemes, excitation energies, spin-parity assignments, and γ-ray transition multipolarities. These data, together with recoil-distance measurements of lifetimes, provide information also on transition strengths for the deexcitation γ rays. Our results suggest assignments of 6^+ and 7^+ for ^{42}K levels at 1376 and 1948 keV, respectively, and indicate higher-lying levels of presumably greater spin. In ^{42}Ca, new odd-parity levels from 6^- to 11^- are proposed as arising from the $d_{3/2}{}^{-1}f_{7/2}{}^3$ configuration.

NUCLEAR REACTIONS: ^{26}Mg(^{18}O,$pn\gamma\gamma\cdots$) E=20–60 MeV, ^{27}Al(^{18}O,$2pn\gamma\gamma\cdots$) E=20–60 MeV; measured γ-γ coin.; deduced levels in ^{42}K, ^{42}Ca; measured $\sigma(E_\gamma,\theta)$ and P_γ; deduced J^π for high-spin levels; measured recoil distance; deduced $T_{1/2}$, $|M(ML)|^2$; confirming evidence from ^{19}F bombardment of ^{26}Mg and ^{28}Si. Enriched targets, Ge(Li) detectors.

I. INTRODUCTION

In systematic investigations[1-5] of the γ rays emitted following the fusion-evaporation reactions induced by bombardment of ^{24,26}Mg, ^{27}Al, and ^{28}Si targets with ^{14}N, ^{16,18}O, and ^{19}F beams, seven γ rays were assigned to transitions in ^{42}K and 19 to transitions in ^{42}Ca. The ^{42}K γ rays were observed in the ^{26}Mg(^{18}O,np)^{42}K, ^{26}Mg(^{19}F,$n2p$)^{42}K, and ^{27}Al(^{18}O,$n2p$)^{42}K reactions while the ^{42}Ca γ rays were observed with the second and third target-projectile combinations and also in the ^{28}Si(^{19}F,$p\alpha$)^{42}Ca reaction.

In this report we present the decay schemes and nuclear structure information obtained for ^{42}K and ^{42}Ca in these investigations. A preliminary report of this work has been given previously.[6] The experimental procedures have been fully discussed.[1-5] Details of γ-ray relative intensities, angular distributions, and excitation functions have been tabulated,[3] as have results of γ-ray linear polarization measurements.[4] We now collect these tabulated results,[3,4] together with such additional data as will be subsequently introduced, in order to examine the description of ^{42}K and ^{42}Ca which emerges.

II. EXPERIMENTAL RESULTS

Table I provides a summary of typical γ-γ coincidence results obtained in the ^{18}O+^{26}Mg bombardment at E(^{18}O)=36 MeV. The measurement utilized two Ge(Li) detectors for γ-ray detection, with the individual coincident events corresponding to an 8192×8192 channel matrix stored on magnetic tape for subsequent analysis. In Table I, we indicate the γ rays observed by one detector in coincidence with sharp γ-ray lines viewed by the other. The considerations leading to the assignment of individual γ rays to a specific final nucleus have been discussed previously.[1-5]

The placement of γ rays assigned to ^{42}K into the ^{42}K decay scheme of Fig. 1 is based on such γ-γ coincidence data (which was taken for all four target-projectile combinations), on the relative intensities observed in singles measurements,[3] and on previous information.[7] ^{42}Ca was not formed in the ^{18}O+^{26}Mg reaction, but similar data from the three remaining reactions result in the level scheme shown in Fig. 2. Examples of γ-γ coincidence data from the ^{18}O+^{26}Mg and ^{18}O+^{27}Al reactions, which provided the most useful information on ^{42}K and ^{42}Ca, respectively, are shown in Figs. 3 and 4.

Information on the lifetimes of these levels was obtained from recoil-distance measurements (RDM) in the ^{18}O+^{27}Al reaction at 35 and 40 MeV, using procedures that have been fully described previously.[1-5] Typical data for ^{42}K and ^{42}Ca are illustrated in Fig. 5.

A. Results for ^{42}K

Decay scheme and lifetime data

Results of lifetime measurements are given in Table II together with branching ratios, transition strengths, and the multipolarities deduced from the linear polarization measurements[4] and the life-

TABLE I. Results of γ-γ coincidences from the ^{26}Mg(^{18}O, xn, yp, zx) reaction.

Gate γ-ray in gate (keV)	Nucleus	Reaction products	Coincident γ rays (keV)
105.92(10) + 106.85(15)	^{38}Ar; ^{42}K	$2n\alpha$; n,p	151, 441, 572, 670, 677, 776, 1643, 1823, 2168
151.24(10)	^{42}K	n,p	107, 441, 572, 677, (992), 1044, 1612
168.39(10)	^{41}Ca	$3n$	460, 545, 1389, 1607, 3201
246.53 (7)	^{41}K	$2n,p$	708, 850, 1123, 1500, 1677
389.71(15)	^{25}Mg	Transfer	585
440.83(20)	^{42}K		107, 151, 572, 677, (992), 1044, 1612
460.27(10)	^{41}Ca		168, 1389, 1607, 3201, 3369
484.50(40)	^{39}Cl	p, α	410
545.48(15)	^{41}Ca	$3n$	168, 3201
551.08(10)	^{39}Ar	n, α	992, 1341, 2651
572.00(30)	^{42}K		107, 151, 441, 677, 1044, 1612
585.12 (9)	^{25}Mg		390
669.87 (8)	^{38}Ar		106, 1643, 1823, 2168
676.95(20)	^{42}K		107, 151, 441, 572, (992), 1044, 1612
708.46(15)	^{41}K		247, 850, 1294, 1468, 1500, 1513, 1677
850.43(10)	^{41}K		247, 708, 1123, 1500, 1677
1043.55(50)	^{42}K		(107), 151, (441), 572, 677
1122.99(50)	^{41}K		247, 850, 1677
1293.64 (4)	^{41}K		708, 1468, 1513
1340.90(20)	^{39}Ar		551, 992, 2651
1389.21(25)	^{41}Ca		168, 460, 1607, 3201
1468.15(15)	^{41}K		708, 1293, 1513
1500.09(25)	^{41}K		247, 708, 850, 1677
1512.78(15)	^{41}K		708, 1293, 1468
1607.24(40) + 1612.15(20)	^{41}Ca; ^{42}K		107, 151, 169, 441, 460, 572, 677, 1389
1642.64(30)	^{38}Ar		106, 670, 775, 1823, 2168
1677.22(20)	^{41}K		247, 708, 850, 1123, 1500
1991.15(30)	^{35}S		Nothing apparent
2167.53 (5)	^{38}Ar		106, 670, 775, 1643, 1823
2651.02(25)	^{39}Ar		551, (992), 1341
3200.85(20)	^{41}Ca		168, 460, 545, 1389, 1607
3369.24(22)	^{41}Ca		460, 545, 1389, (1607)

time measurements. Transition strengths are given in the conventional[8] Weisskopf units (W.u.).

The γ-ray decay of the three levels below 700-keV excitation (see Fig. 1) have been previously well established[7] and thus provide a basis for interpreting the γ-γ coincidence data of Table I. The placement of the 677- and 572-keV transitions in the level scheme of Fig. 1 is unambiguous. The 1612- and 1044-keV γ rays were observed only in the ^{26}Mg(^{18}O, np)^{42}K coincidence data and because of intensity limitations it was not possible to determine whether or not they were in coincidence with each other. The 1612-keV γ ray was the more intense, hence the ordering we have indicated.

The 572- and 1612-keV γ rays were unresolved from γ rays of nearly identical energies. In detail, we have observed unambiguous evidence from the γ-γ coincidence data for a ^{43}Ca γ ray of 572.64 $\pm$0.20 keV and an ^{40}Ar γ ray of 572.20$\pm$0.50 keV, both of which are evident in the ^{18}O + ^{27}Al and ^{19}F + ^{26}Mg data. We expect contributions to the 572-keV peak from ^{40}Ar and ^{43}Ca to be smallest in the ^{18}O + ^{26}Mg reaction, since these nuclei are formed through decay of the compound nucleus ^{44}Ca by single neutron and single α-particle emission, respectively, and these cross sections are relatively very weak. This is borne out by the γ-γ coincidence data in which no ^{43}Ca and only very weak ^{40}Ar γ rays are seen in coincidence with the 572-keV peak observed in the ^{18}O + ^{26}Mg reaction.

In all three reactions studied, the ^{42}K γ ray of 1611.97$\pm$0.30 keV is obscured by the γ ray at 1611.24$\pm$0.09 keV[7] resulting from the decay of the first-excited state of ^{37}Ar and from a contaminant γ ray at 1611.50$\pm$0.50 keV from the ^{25}Mg 1612 $\rightarrow$ 0 transition following formation via reactions induced on ^{12}C and ^{16}O contaminants. Thus, for both the 572- and 1612-keV γ rays of ^{42}K the relative intensities can be only very roughly estimated from the coincidence data and excitation functions.

We note in passing that the ^{40}Ar 572-keV γ ray was observed in coincidence with the well known[7]

$4^+ \to 2^+ \to 0^+$ cascade γ rays in ^{40}Ar of energies 1431.66 ± 0.20 and 1460.90 ± 0.20 keV, respectively. These data therefore indicate a new level in ^{40}Ar at 3464.80 ± 0.54 keV, based on a value of 2892.60 ± 0.20 keV for the excitation energy of the 4^+ level.[7] [*Note added in proof:* Flynn, Hansen, Casten, Garrett, and Ajzenberg-Selove[8(a)] recently reported a probable 6^+ ^{40}Ar level at an excitation energy of 3468 ± 5 keV observed via the $^{38}Ar(t,p)^{40}Ar$ reaction.] Likewise, the ^{43}Ca 572-keV γ ray corresponds to the γ decay of a previously unobserved level at 3943.82 ± 0.45 keV which decays to the level reported at 3372 keV,[7] which we place at 3371.20 ± 0.40 keV. From RDM measurements utilizing $^{19}F + ^{27}Al$ we find the ^{43}Ca 3944-keV level has a mean life less than 5 psec.

Because of the experimental difficulties mentioned above, no lifetime information was obtained from the 1044- and 1612-keV γ rays and only a limit was obtained from the 572-keV γ ray. The intensity of the 572-keV γ ray decayed with plunger displacement with an apparent mean life of 750 ± 200 psec. Since the ^{43}Ca 572-keV γ ray will decay with $\tau_m \leq 5$ psec, the 750-psec mean life is due to the ^{42}K or ^{40}Ar γ rays or a combination of both; hence the limit. The RDM measurement on the 677-keV γ ray was straightforward. The uncertainty includes the uncertainty generated by feeding from a level of ill-determined lifetime. In $^{18}O + ^{27}Al$ the 699-keV level is fed almost entirely by cascade from the 1376-keV level. Thus, the effect of its meanlife was largely obscured and only a limit could be obtained. The 151-keV γ ray (see Fig. 5) had an RDM decay curve characteristic of two components—delayed cascade via the 1100-psec 1376-keV level and relatively prompt feeding via the 699-keV level and directly from the reaction. The least-squares fit also indicated a long-

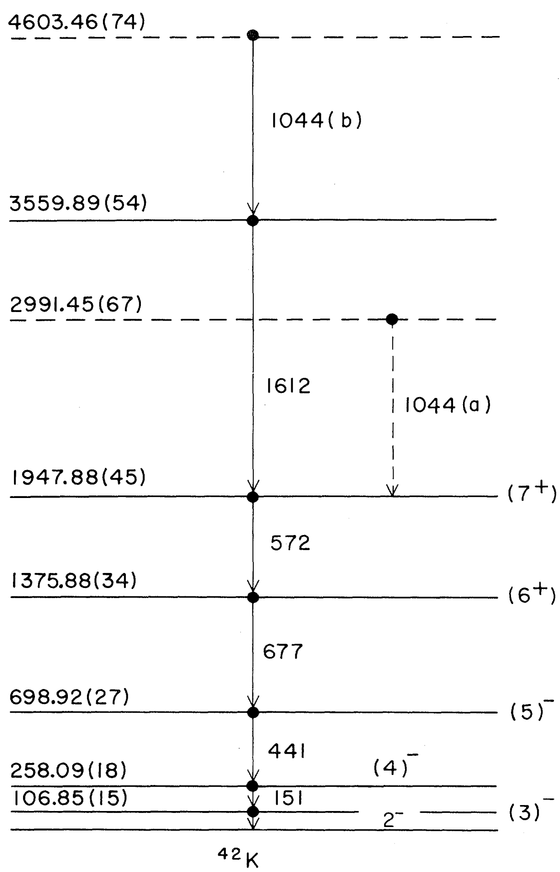

FIG. 1. Decay scheme for high-spin states in ^{42}K. The level energies, which are in keV with the uncertainties in parentheses, are from the present γ-ray energy measurements (Ref. 3) and include the γ-ray recoil correction. The spin-parity assignments for the states below 700 keV are from Ref. 7; the others are discussed in the text. The two possible placements of the 1044-keV γ ray are shown. All observed ^{42}K γ rays are shown.

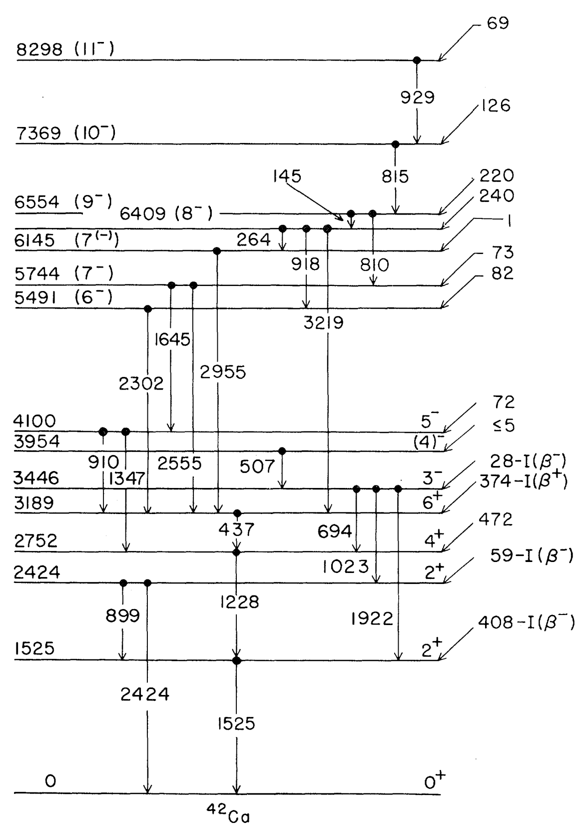

FIG. 2. Decay scheme for high-spin states in ^{42}Ca. The spin-parity assignments for levels below 5 MeV are from Ref. 7; the others are discussed in the text. The relative intensities for feeding the various levels in the $^{27}Al(^{18}O, 2np)^{42}Ca$ reaction at 40 MeV are given on the right. The $I(\beta^{\pm})$ refer to the unknown feeding intensities from $^{42}K(\beta^-)$ and $^{42}Sc^m(\beta^+)$ decays (see Ref. 7). Level and γ-ray energies are in keV. Branching ratios and accurate excitation energies are given in Table IV.

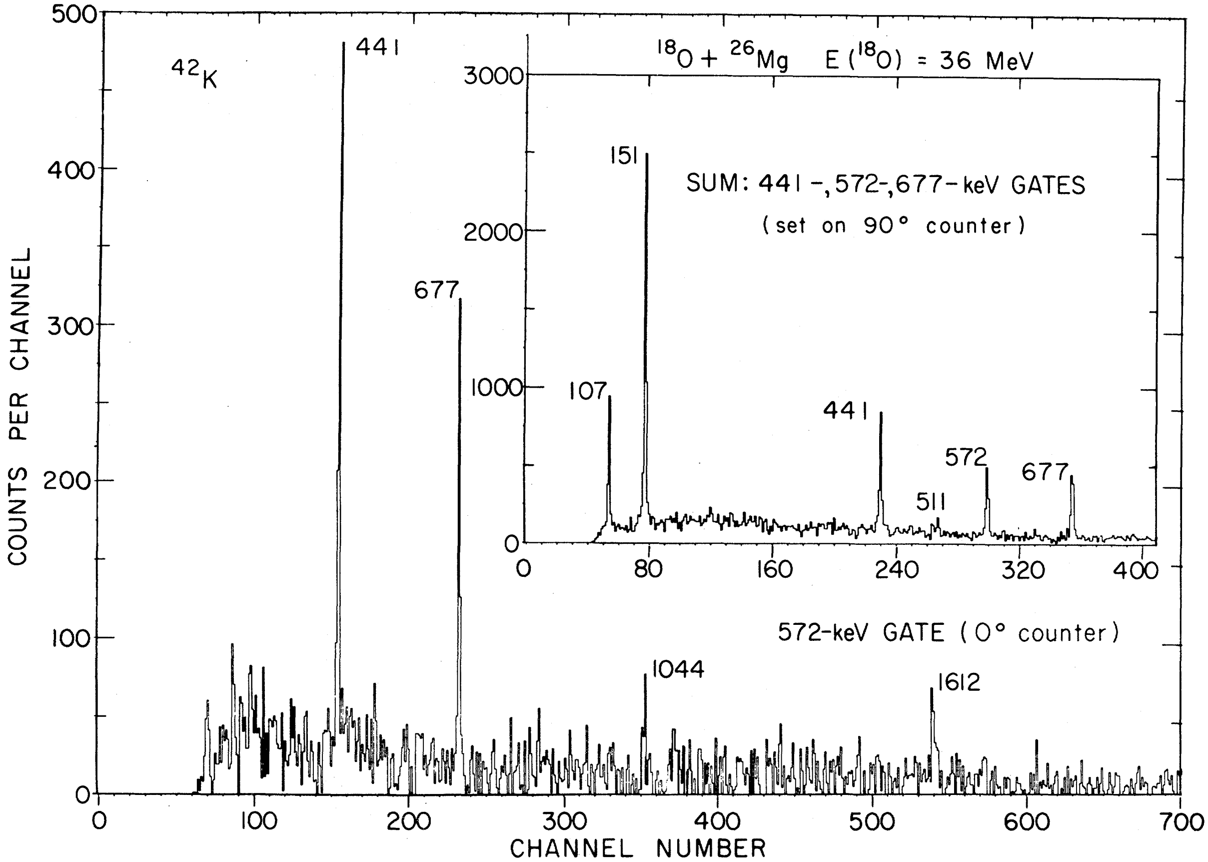

FIG. 3. Typical coincidence spectra from ^{18}O + ^{26}Mg at 36 MeV. These data establish the existence of four new transitions in ^{42}K.

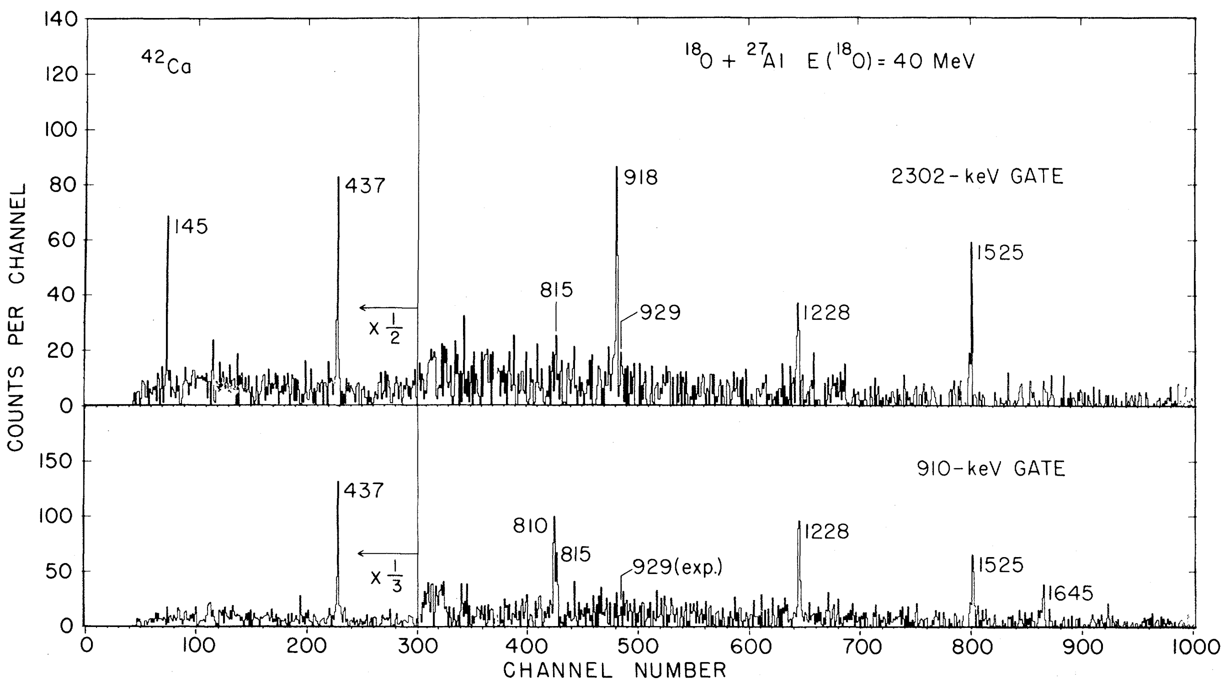

FIG. 4. Typical coincidence data from ^{18}O + ^{27}Al at 40 MeV.

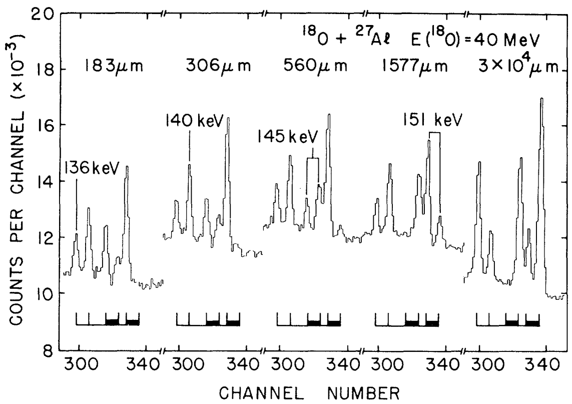

FIG. 5. RDM results at five different target-plunger displacements (183 to 3×10^4 μm). The 136- and 140-keV γ rays are from ^{181}Ta and ^{75}Ge, respectively (Ref. 3), while the 145- and 151-keV γ rays are from ^{42}Ca and ^{42}K, respectively (see Figs. 1 and 2). The positions of the six observed peaks are indicated below the spectra. The fiducial marks for the stopped (I_0) and shifted (I_s) peaks of the 145- and 151-keV lines are connected by broad horizontal lines. To first order the ratio $I_0/(I_0+I_s)$ decays exponentially with the plunger-target distance as $\exp(-D/v\tau)$, where v is the recoil velocity and τ the meanlife of the decaying level.

lived component which we ascribe to the decay of the ^{43}Sc 151.7-keV first-excited state[7] formed via the ^{27}Al(^{18}O, $2n$)^{43}Sc reaction.

γ-ray angular distribution and polarization measurements

For highly aligned states as are produced in fusion-evaporation reactions, the angular distribution and linear polarization data exhibit a convenient signature for stretched quadrupole or dipole transitions, i.e., for transitions $J_i \to J_f$ with $J_f = J_i \pm L$. A satisfactory treatment of the general problem is given by Yamazaki,[9] in which the initial alignment is parametrized in terms of a Gaussian distribution of substates centered at $m_J=0$, with a width which in the present work is given by $\sigma \sim (0.4\pm0.2)J$. The observed experimental angular distributions are simply related to those expected for full alignment by attenuation coefficients α_2 and α_4, which describe the attenuation of the a_2 and a_4 coefficients of the Legendre polynomial fit. As indicated previously,[4] the linear polarization $P(ML)$ for a stretched transition of multipolarity ML is readily calculated from the coefficients a_2 and a_4.

For both ^{42}K and ^{42}Ca the experimental angular distributions agree with those expected for the spins indicated in Figs. 1 and 2, if we assume a smooth variation of σ within the range $0.2 \leq \sigma/J \leq 0.6$, with the smaller value appropriate for the highest-lying excited state. With this variation we have the following expectations, which appear consistent with experiment: For pure dipole transitions, $-0.2 \gtrsim a_2 \gtrsim -0.3$, with $a_4 \equiv 0$, which leads to a prediction[4] for $M1$ radiation $P(M1) \sim -(0.33 \pm 0.06)$. For pure quadrupole transitions, $+0.2 \lesssim a_2 \lesssim 0.4$, and $-0.05 \gtrsim a_4 \gtrsim -0.15$, with a predicted polarization for $E2$ radiation $P(E2) \sim +(0.48\pm0.18)$. The predicted polarization for parity-changing $E1$ and $M2$ radiations are of the same magnitude but opposite sign.[4]

As discussed previously,[1,2,4,5] the predictions indicated above are "model dependent" in the sense that the calculations assume a significant alignment for the initial state. However, for cases where it is known that the transition is pure dipole or quadrupole (or alternately, J_i, J_f, and the mixing ratio are known), the polarization may be determined exactly from the experimental a_2 and a_4 coefficients.

With these general considerations in mind, we now turn to an examination of the pertinent data for ^{42}K which is summarized in Table III. The angular distributions obtained[3] for the 151-, 441-, 572-, and 677-keV transitions are all in agreement

TABLE II. Summary of results for ^{42}K.

E_i (keV)	E_f (keV)	E_γ (keV)	τ_m (psec)	Multipolarity	Transition strength [a] (W.u.) Dipole	Quadrupole	$J^\pi{}_i$	$J^\pi{}_f$
106.85	0	107	370± 160 [b]	$M1$ [c]	0.07	18×10^3	3^-	2^-
258.09	106.85	151	170± 40	$M1$ [c]	0.05	7×10^3	4^-	3^-
698.92	258.09	441	<20	$M1$	>0.02	>276	5^-	4^-
1375.88	698.92	677	1100± 300	$E1$	2.3×10^{-6}	23	6^+	5^-
1947.88	1375.88	572	≤750± 200	$M1$	$\geq2.2\times10^{-4}$	≥2	7^+	6^+

[a] τ_m (Weisskopf)/τ_m (experimental), where τ_m (Weisskopf) is given by D. H. Wilkinson (Ref. 8). The uncertainties on the transition strength derive from those on the τ_m. The strengths for quadrupole radiation are for pure quadrupole radiation with the mean life and parity change indicated.

[b] From Ref. 7.

[c] These multipolarities follow from the odd parity assigned to the initial and final states (Ref. 7) and from the transition strengths.

with those expected for $J+1 \rightarrow J$ dipole transitions. Linear polarizations of the 441-, 572-, and 677-keV transitions were measured for both $^{18}O + ^{26}Mg$ and $^{18}O + ^{27}Al$. The two sets of data are in good agreement and are consistent with pure dipole radiation with the multipolarity listed in Table II. With reference to the $^{18}O + ^{26}Mg$ results of Table III, the measured linear polarizations clearly indicate $M1$ character for the 441- and 572-keV transitions. The data on the 677-keV transition are considered not definitive, and we have included the results from the $^{18}O + ^{27}Al$ measurements, which indicate clearly that the transition is $E1$, i.e., parity changing.

For both the 441- and 572-keV transitions, the lifetime limits restrict any possible $M2$ contributions sufficiently that the linear polarization measurements can be used to rule out a parity charge. For the 677-keV transition the data do not rule out an $M1, E2$ mixture, but essentially pure $E1$ radiation gives good agreement with the angular distribution and linear polarization measurements and is considered most probable.

The most probable spin-parity assignments of 6^+ and 7^+ for the 1376- and 1948-keV levels (see Fig. 1) follow from the multipolarities listed in Table II and the argument that the fusion evaporation reaction strongly selects yrast levels.[1-5] Additional evidence for these assignments comes from the $^{40}Ar(\alpha, d)^{42}K$ results of Kouzes and Sherr[10] who assigned 7^+ to a 1950-keV level observed in this reaction.

TABLE III. ^{42}K γ-ray data from $^{26}Mg(^{18}O, np)^{42}K$ at $E(^{18}O) = 40$ MeV.

E_γ [a] (keV)	Relative[b] intensity	Angular distribution[c] a_2 (%)	a_4 (%)	Linear polarization Exp.[d]	Pred.[e]
572.00(30)	2912	−44(4)	0	−36(10)	−47(6)
676.95(20)	2757	−37(4)	0	8(11)	−46(6)
		−16(4)[f]	0[f]	28(13)[f]	−22(7)[f]
440.83(20)	4091	−16(3)	0	−44(12)	−22(5)
151.24(10)	6504	−19(4)	0	···	···

[a] γ-ray energies are from Ref. 3.
[b] Intensities corrected for detector efficiency.
[c] Reference 3. The Legendre polynomial coefficients are in percent, with $a_0 \equiv 1$.
[d] Experimental polarization in percent, from Ref. 4.
[e] Predicted polarization in percent, from Ref. 4. The polarization is calculated from the experimental angular distribution assuming pure $M1$ or $E2$ radiation. The opposite sign would obtain for pure $E1$ or $M2$ radiation. The prediction is not valid for mixed transitions or for pure multipoles with $L > 2$.
[f] Results from $^{27}Al(^{18}O, 2pn)^{42}K$ at $E(^{18}O) = 40$ MeV.

B. Results for ^{42}Ca

Whereas the levels below 5-MeV excitation (see Fig. 2) have been observed in a number of light-ion reactions,[7] the higher-lying levels have been observed only in heavy-ion fusion-evaporation reactions. The states which we observe from the reactions cited in this report have also been seen in the $^{28}Si(^{16}O, 2p)^{42}Ca$ reaction by Wüst *et al.*[11] and independently by Kim, Robinson, and Milner.[12] The γ-ray angular distribution,[3] linear polarization,[4] and lifetime results are summarized in Tables IV and V. When coupled with the arguments for selective feeding of yrast levels, these data lead to the proposed spin-parity assignments indicated in Fig. 2 and Table IV.

The lifetime measurements for the three highest-lying levels were straightforward. Typical data illustrating the 145-keV 6554 → 6409 transition is shown in Fig. 5. For the lower-lying levels our results were in some cases ambiguous, because of complicated cascade feeding, but they are in general consistent with the RDM measurements of Wüst *et al.*[11] The mean lives which we have determined are summarized and compared to other measurements in Table IV. The mean life for the 2752-keV level has been reported previously.[13]

The arguments leading to the suggested spin-parity assignments of Fig. 2 are not based solely on the data of Tables IV and V, but rely heavily on the argument that the heavy-ion reaction should populate most strongly the yrast levels; i.e., the levels populated correspond to the lowest-lying levels of a given spin and parity. With this argument the weak population of the 6145-keV level ($J = 7$) can be explained in a plausible manner, in that the major feeding takes place to a lower-lying level of $J = 7$. In the following discussion, we shall not belabor this point. Rather, we shall examine the extent to which the various data are in agreement with, and thus support, the level scheme we have proposed in Fig. 2.

Even-parity levels $E_x < 3.3$ MeV

The spin-parity assignments and decay schemes indicated in Fig. 2 are well established from reports cited previously.[7] The results which we report here provide confirmation for these conclusions: more important, they allow us to assess the quality of the data presented in Table V, which are of interest to the discussion of higher-lying levels of ^{42}Ca. The angular distributions measured for the 437-, 1228-, and 1525-keV γ rays, corresponding to the $6^+ \rightarrow 4^+ \rightarrow 2^+ \rightarrow 0^+$ cascade transitions, are individually characteristic of stretched quadrupole transitions from highly aligned states ($a_2 \sim 0.23$ and $a_4 \sim -0.12$). As can be seen from Table V, the measured polarizations are in excellent accord

TABLE IV. Summary of results for ^{42}Ca.

E_i [a] (keV)	E_f (keV)	E_γ (keV)	B.R. [b] (%)	τ_m (psec) Other [f]	τ_m (psec) Present	τ_m (psec) Adopted	Multipolarity [c]	Transition strength [d] (W.u.) Dipole	Transition strength [d] (W.u.) Quadrupole	J^π_i [e]	J^π_f [e]
8297.88(40)	7369	929	100		<2.5	<2.5	$M1$	>0.016	>53	11^-	10^-
7368.78(34)	6554	815	100	2.2 ± 1.1	3.7 ± 1.6	3.0 ± 1.4	$M1$	0.019	85	10^-	9^-
6554.02(30)	6409	145	24 ± 4	63.2 ± 9.5	61 ± 4	61 ± 4	($M1$)	0.039	5500	9^-	8^-
	5744	810	76 ± 4				$E2$	...	3.3	9^-	7^-
6408.90(33)	6145	264	17 ± 3	44.8 ± 3.6		44.8 ± 3.6	($M1$)	0.006	273	8^-	$7^{(-)}$
	5491	918	70 ± 2				$E2$	...	2.2	8^-	6^-
	3189	3219	13 ± 2				{($M2$) [g]	...	0.03	8^-	6^+
							{($E3$) [g]	...	1.1 ± 0.3 [g]		
6145.05(33)	3189	2956	100				($E1$)	...	...	$7^{(-)}$	6^+
5744.20(28)	4100	1645	51 ± 2	15.2 ± 1.4		15.2 ± 1.4	($E2$)	...	0.26	7^-	5^-
	3189	2555	49 ± 2				($E1$)	1.5×10^{-6}	1.08	7^-	6^+
5491.09(30)	3189	2302	100		<2.5	<2.5	$E1$	$>2.6\times10^{-5}$	>22	6^-	6^+
4099.69(20)	3189	910	61 ± 2 [h]	<1.0		<1.0	$E1$	$>6\times10^{-4}$	>3500	5^-	6^+
	2752	1347	33 ± 2 [h]				($E1$)	$>1\times10^{-4}$	>270	5^-	4^+
3953.70(120)	3446	507	100				($M1$)			$(4)^-$	3^-
3571.58(17) [i]	3189	582	100			...	?	...	...	?	6^+
3446.43(80) [i]	1525	1922	60 ± 2	0.36 ± 0.14		0.36 ± 0.14	$E1$	1.9×10^{-4}	230	3^-	2^+
3253.86(40)	2752	502	35 ± 5	0.19 ± 0.03		0.19 ± 0.03	$M1$	0.46	5340	4^+	4^+
3189.33(14)	2752	437	100	7790 ± 130		7790 ± 130	$E2$	...	0.74	6^+	4^+
2752.29(11)	1525	1228	100	3.8 ± 0.4	5.1 ± 0.4	4.6 ± 0.3	$E2$	...	7.2	4^+	2^+
2423.61(22)	1525	899	70 ± 1	0.20 ± 0.06		0.20 ± 0.06	$M1$	0.15	548	2^+	2^+
1524.61 (8)	0	1525	100	1.19 ± 0.04		1.19 ± 0.04	$E2$	...	9.4	2^+	0^+

[a] From the γ-ray energy measurement of Ref. 3. The uncertainty assigned to the last figure is given in parentheses.

[b] The branching ratios (B.R.) for all levels below 3.5-MeV excitation, except the 2752-keV level, are from Ref. 7.

[c] From the linear polarization (Ref. 4) and lifetime measurements. For those multipolarities in parentheses, linear polarization measurements were either not available or not definite.

[d] τ_m (Weisskopf)/τ_m (experimental) (B.R./100), where τ_m (Weisskopf) is given by D. H. Wilkinson (Ref. 8). The uncertainties on the transition strengths derive from those on the τ_m and branching ratios. The strengths for quadrupole radiation are for pure quadrupole radiation with the mean life and parity change indicated.

[e] The spin-parity assignment for all levels below 5-MeV excitation are from Ref. 7. For $E_x > 5$ MeV the assignments are from the present work and are most probable rather than definite.

[f] Lifetime measurements for $E_x > 4$ MeV are from Ref. 11. Results for $E_x < 4$ MeV are from Ref. 7.

[g] Strengths correspond to an $E2/M2$ mixing ratio $x = +0.3 \pm 0.1$; the corresponding $E3$ strength is given in Col. 10.

[h] Assumes a 6% branch to the 3446-keV level (see Ref. 7).

[i] Due to the low intensity of the deexcitation γ ray, there is some doubt as to the population or existence of this level.

TABLE V. ^{42}Ca γ-ray data from ^{27}Al(^{18}O, $2np$)^{42}Ca at E(^{18}O) = 40 MeV.

E_γ [a] (keV)	Relative [b] intensity	Angular distribution [c] a_2 (%)	a_4 (%)	Linear polarization Exp. [d]	Pred. [e]
929.10(25)	6920	−25 (7)	0	−67(27)	−33(10)
814.75(15)	19488	−30 (6)	−2 (4)	−41 (9)	−40 (9)
809.88(12)	32253	30 (3)	−19 (3)	37 (8)	42 (8)
263.74(15)	4674	−18 (2)	−14 (3)	···	···
917.87(12)	24057	31 (5)	−17 (5)	41(12)	45(13)
3219.29(60)	4484	72 (5)	0	···	···
2955.60(30)	4800	−30 (8)	0	···	···
1644.54(20)	22202	26 (2)	−17 (3)	25(29)	35 (6)
2544.70(25)	17355	−26(16)	0	−17(30)	−34(20)
2301.68(25)	32345	32 (3)	−10 (4)	−30(25)	52 (8)
910.45(15)	19185	−20 (2)	−7 (3)	19 (9)	−32 (5)
1347.24(20)	10192	−23 (2)	0	5(25)	−42 (5)
382.24(10)	2802	−42(12)	0	−52(15)	−52(14)
1921.77(80)	2191	−55(14)	0	···	···
437.04 (8)	118368	23 (2)	−15 (2)	32 (5)	30 (6)
1227.66 (8)	176595	23 (1)	−11 (1)	29 (6)	32 (4)
898.99(20)	4986	13(10)	11(15)	···	···
1524.58 (8)	222453	22 (1)	−10 (1)	37 (9)	31 (4)

[a] Only those ^{42}Ca transitions for which angular distribution and/or linear polarization results were obtained are listed. Energies are from Ref. 3.

[b] Intensities corrected for detector efficiency. The estimated accuracy of the relative yields for two intense lines varies with their energy separation from ≲1% to ~15%. For weak lines, the uncertainty may be as much as 50%.

[c] Reference 3. The Legendre polynomial coefficients are in percent, with $a_0 \equiv 1$.

[d] Experimental polarization in percent, from Ref. 4.

[e] Predicted polarization in percent, from Ref. 4. The polarization is calculated from the experimental angular distribution assuming pure $M1$ or $E2$ radiation. The opposite sign would obtain for pure $E1$ or $M2$ radiation. The prediction is not valid for mixed transitions or for pure multipoles with $L > 2$.

with those expected for pure quadrupole radiation, and the sign of the polarization designates the character unambiguously as $E2$.

The $J^\pi = 2^+$ state at 2424 keV, which is known to decay to the ground and 1525-keV states, was formed only weakly relative to the adjacent even parity states. The ground state transition was not resolved in singles measurements, but the observation of the 899-keV γ ray serves to fix the excitation energy of the 2424-keV level relative to the 1525-keV level to which it decays (see Table IV). Similarly, the 502-keV γ ray corresponding to the 3254 → 2752 transition has been used to fix the energy of the 3254 keV state. This 4^+ level has been omitted, for reasons of clarity, from Fig. 2 since it is not involved in the decay of higher-lying states of interest here.

Levels at 3446, 3954, and 4200 keV

The 3^- state at 3446 keV is known[7] to branch to the lower-lying 2^+ and 4^+ states. The decays to the two 2^+ states were observed in the γ-γ coincidence data but the 694-keV transition was not, presumably because of the small branching ratio (4%)[7] and the relatively weak population of the state. Only the 1922-keV γ ray was clearly resolved in singles; the measured angular distribution is in accord with that expected for a stretched dipole transition.

The 5^- level at 4100 keV decays to the lower-lying 4^+ and 6^+ states. The angular distributions for both the 910-keV ($5^- \to 6^+$) transition and the 1347-keV ($5^- \to 4^+$) transition are in good accord with pure dipole radiation. The polarization measurements on the 910-keV γ ray define $E1$ character for this transition, in agreement with an odd-parity assignment for the 4100-keV level. The polarization data on the 1347-keV transition involve much larger errors, and are considered not definitive.

An odd-parity level has been reported from light-ion studies (as summarized in Ref. 7) at 3949 ± 7 keV, with a most probable spin $J = 4$. The state is known[7] to decay predominantly (>60%) to the 3446 ($J^\pi = 3^-$) state, and thus we associate the state with the level we observe at 3953.7 ± 1.2 keV (see Table IV). The 507.3 ± 0.9 keV γ ray, resulting from the decay of this level to the 3446-keV (3^-) level, was observed only in coincidence with the decay γ rays from the 3446 keV level. It could not be seen in singles measurements due to much stronger 502- and 511-keV γ rays. The observation of the 3954-keV level in the ^{18}O + ^{27}Al reaction lends support to the $J = 4$ assignment, on the grounds that the transition is most likely dipole from a level of $J > 3$.

Levels with $E_x > 5$ MeV

5491-keV level. The angular distribution of the 2302-keV γ ray has a positive a_2 coefficient, in agreement with a $J \to J$ dipole transition corresponding to the spin sequence $6^- \to 6^+$ which we have suggested (Fig. 2) as based on all the available information. The linear polarization defines the character as $E1$, if pure dipole, strongly supporting an odd-parity assignment for the initial level.

5744-keV level. The 1645-keV transition to the 4100-keV (5^-) level exhibits the strong angular distribution and polarization effects characteristic of stretched $E2$ radiation, in agreement with our suggestion of $J^\pi = 7^-$ for the 5744-keV level. The angular distribution measured for the 2555-keV transition (with $a_2 = -26\%$) agrees well with pure dipole radiation. In this case the transition must be $E1$, but the linear polarization results are not definitive because of larger experimental errors.

6145-keV level. Little information could be obtained on this level. The angular distribution of the 2955-keV decay to the 3189-keV 6^+ level is consistent with the suggested 7^- assignment.

6409-keV level. In this case the most useful information is contained in the 918-keV γ ray leading to the 5491 (6^-) state. The measured angular distribution and polarization characterize unambiguously a stretched $E2$ transition, consistent with the suggested 8^- assignment for the initial state. The angular distribution measured for the 264-keV transition to the 6145-keV level does not correspond to that expected for a pure dipole transition, thus suggesting a possible mixing in this transition. This is in accord with the suggested $7^{(-)}$ assignment for the 6145-keV level, since the mixing in this case would be $E2/M1$.

Finally, the 3219-keV transition to the 3189-keV 6^+ level exhibits the large a_2 coefficient and small a_4 coefficient which characterize a mixed $E3/M2$ transition. The measured distribution can be fitted for a mixing ratio $x=+(0.3\pm0.1)$, where we have assumed a Gaussian spreading of substates characterized by $\sigma=0.25J$, which was deduced primarily from similar fits to data on the stretched quadrupole and dipole transitions evident in Table V.

6554-keV level. The data on the 810-keV transition to the 5744-keV (7^-) level are in excellent agreement with that expected for a stretched $E2$ cascade, leading to a suggested assignment $J^\pi=9^-$ for the 6554-keV level. No angular distribution information was obtained for the low-energy 145-keV transition.

7369- and 8298-keV levels. For both these levels, the deexcitation γ rays exhibit angular distributions characteristic of stretched dipole radiation (large negative a_2 coefficients), together with linear polarizations characteristic of $M1$ radiation. The data are therefore in good accord with the 10^- and 11^- spin-parity assignments we have suggested in Fig. 2.

III. DISCUSSION

It is expected that the high-spin states observed in the present work on $A=42$ belong predominantly to $(d_{3/2})^{-n}(f_{7/2})^{2+n}$ configurations. The odd-parity states of both ^{42}K and ^{42}Ca would then be $(d_{3/2})^{-1}(f_{7/2})^3$, while the lowest-lying even-parity states would be $(d_{3/2})^{-2}(f_{7/2})^4$ in ^{42}K and $(f_{7/2})^2$ in ^{42}Ca. The ^{42}K odd-parity levels are seen to arise simply from $[d_{3/2}(\pi)^{-1}f_{7/2}(\nu)]\cdot[f_{7/2}(\nu)^2]_{0^+}$, which generates the observed 2^-, 3^-, 4^-, 5^- sequence. The similarity to the $d_{3/2}(\pi)^{-1}f_{7/2}(\nu)$ levels[7] of ^{40}K is easily apparent.

The observed 0^+, 2^+, 4^+, 6^+ sequence of states in ^{42}Ca exhausts the levels which can be formed from the $(f_{7/2})^2$ configuration. The odd parity levels can be enumerated by the coupling of $(d_{3/2})^{-1}f_{7/2}$ (which generates the 2^-, 3^-, 4^-, 5^- odd-parity spectrum seen for example in ^{42}K) to the even-parity states of $(f_{7/2})^2$ as described above. The resultant $[(d_{3/2})^{-1}f_{7/2}]\otimes[(f_{7/2})^2]$ configuration gives rise to states $1^-\leq J^\pi\leq 11^-$, with multiple states for each $J<11$. For example, the 3^-, 4^-, 5^- states of Fig. 2 presumably arise from $[(d_{3/2})^{-1}f_{7/2}]_{J\pi}\otimes[(f_{7/2})^2]_{0^+}$; the $J^\pi=2^-$ state has apparently been missed. The 6^- and 7^- states then correspond to the two highest spin states formed from $[(d_{3/2})^{-1}f_{7/2}]_{J\pi}\otimes(f_{7/2})_{2^+}$; the lower spin states are not yrast states and are thus not fed significantly in the heavy ion reaction. Similar couplings to $[(f_{7/2})^2]_{4^+}$ and $[(f_{7/2})^2]_{6^+}$ generate the remaining 8^-, 9^-, and 10^-, 11^- grouping of yrast states, respectively, although the 9^- state could also be obtained from the $[(f_{7/2})^2]_{6^+}$ coupling. While admittedly crude, this picture gives a reasonable projection for the spin sequence and level spacing observed in ^{42}Ca. In particular, the relatively large separation of the 5^- and 6^- states is seen to correspond very closely to that of the 0^+ and 2^+ states on which they are respectively based.

Additional data supporting the suggested configurations is evident from the transition strengths which have been determined for ^{42}K and ^{42}Ca. For example, $E1$ transitions are forbidden between $(d_{3/2})^{-n}(f_{7/2})^{2+n}$ states, since the $\langle d_{3/2}|E1|f_{7/2}\rangle$ matrix element is identically zero. Thus the model space proposed gives a ready explanation for the smallness of the $E1$ transitions listed in Tables II and IV.

In summary, the net evidence on both ^{42}K and ^{42}Ca appears consistent with the description we have proposed. Further discussion should await shell model calculations within $(d_{3/2})^{-n}(f_{7/2})^{2+n}$, or perhaps within an even more extensive configurational space.

The collaboration of A. R. Poletti in early phases of this work is gratefully acknowledged.

†Work performed under the auspices of the U.S. Atomic Energy Commission.

[1]P. Gorodetzky, J. J. Kolata, J. W. Olness, A. R. Poletti, and E. K. Warburton, Phys. Rev. Lett. 31, 1067 (1973).
[2]J. J. Kolata, Ph. Gorodetzky, J. W. Olness, A. R. Poletti, and E. K. Warburton, Phys. Rev. C 9, 953 (1974).
[3]E. K. Warburton, J. J. Kolata, J. W. Olness, A. R. Poletti, and Ph. Gorodetzky, At. Data Nucl. Data Tables 14, 147 (1974).
[4]J. W. Olness, A. H. Lumpkin, J. J. Kolata, E. K. Warburton, J. S. Kim, and Y. K. Lee, Phys. Rev. C 11, 110 (1975).
[5]J. J. Kolata, J. W. Olness, and E. K. Warburton, Phys. Rev. C 10, 1663 (1974).
[6]E. K. Warburton, Ph. Gorodetzky, J. J. Kolata, J. W. Olness, and A. R. Poletti, Bull. Am. Phys. Soc. 19, 75 (1974).
[7]P. M. Endt and C. Van der Leun, Nucl. Phys. A214, 1 (1973).
[8]D. H. Wilkinson in *Nuclear Spectroscopy*, edited by F. Ajzenberg-Selove (Academic, New York, 1960), Pt. B, p. 862ff.
[8(a)]E. R. Flynn, O. Hansen, R. F. Casten, J. D. Garrett, and F. Ajzenberg-Selove, unpublished.
[9]T. Yamazaki, Nucl. Data A3, 1 (1967).
[10]R. Kouzes and R. Sherr, Bull. Am. Phys. Soc. 18, 602 (1973).
[11]N. Wüst *et al.*, J. Phys. (to be published).
[12]H. J. Kim, R. L. Robinson, and W. T. Milner, in *Proceedings of the International Conference on Nuclear Physics, Munich, 1973,* edited by J. de Boer and H. J. Mang (North-Holland, Amsterdam/American Elsevier, New York, 1973).
[13]A. R. Poletti, B. A. Brown, D. B. Fossan, E. K. Warburton, P. Gorodetzky, J. J. Kolata, and J. W. Olness, Phys. Rev. C 10, 997 (1974).